The equilibrium solutions and visualizations to the incompressible fluid ellipsoids

By

RUICONG ZHENG

UNDERGRADUATE THESIS

Submitted in partial satisfaction of the requirements for the degree of

BACHELOR OF SCIENCE

in

MATHEMATICS

in the

COLLEGE OF LETTERS AND SCIENCE

of the

UNIVERSITY OF CALIFORNIA

DAVIS

Approved:

Joseph Biello

Abstract

We show and derive the mathematical contents on understanding the incompressible fluid ellipsoids, which include incompressible fluid dynamics and the matrix form of the dynamics after applying the Dirac brackets and Hamiltonian reduction. Then we talk about the conserved quantities in the system, show the different types of the ellipsoids, and construct the equilibrium solutions for them. We also constructed a programming code to visualize the results.

Contents

1 Historical introduction **3**

2 Mathematical background **3**
- 2.1 Fluid dynamics . . . 3
  - 2.1.1 The derivation of the momentum equation . . . 3
  - 2.1.2 Incompressibility . . . 4
  - 2.1.3 Mass conservation . . . 4
- 2.2 The ordinary differential equations (ODEs) describing the fluid ellipsoids . . . 4
  - 2.2.1 The Hamiltonion/kinetic energy . . . 5
  - 2.2.2 Potential energy . . . 6
  - 2.2.3 The ODEs of the systems . . . 6

3 Conserved quantities **6**
- 3.1 Total energy . . . 6
- 3.2 Kelvin's circulation . . . 7
- 3.3 Total volume . . . 7
- 3.4 Divergence of the velocity field . . . 7

4 The equilibrium solutions **8**
- 4.1 The geometry of different types of ellipsoids . . . 8
  - 4.1.1 Maclaurin spheroids . . . 8
  - 4.1.2 Jacobi ellipsoids . . . 9
  - 4.1.3 Dedekind ellipsoids . . . 10
  - 4.1.4 Riemann ellipsoids . . . 11
- 4.2 Equilibrium solutions . . . 11
  - 4.2.1 Set-up . . . 11
  - 4.2.2 Changing to the rotational frame of reference . . . 12
  - 4.2.3 Equilibrium solutions for Maclaurin spheroids and Jacobi ellipsoids . . . 13
  - 4.2.4 Equilibrium solutions for Dedekind ellipsoids . . . 14

5 Visualization of the ellipsoids and conserved quantities **14**
- 5.1 Conserved quantities . . . 14
- 5.2 Equilibrium of the Maclaurin Spheroid and its dynamics near the equilibrium state . . . 16
- 5.3 Equilibrium of the Jacobi Ellipsoid and its dynamics near the equilibrium state . . . 19

6 Future work **21**

7 Appendix **21**
- 7.1 Main code . . . 21
- 7.2 MatrixToVector function . . . 23
- 7.3 VectorToMatixCell function . . . 23
- 7.4 Get axes function . . . 23
- 7.5 Volume calculation function . . . 24
- 7.6 Plot axes function . . . 24
- 7.7 Gamma calculation function . . . 24
- 7.8 Divergence calculation function . . . 24
- 7.9 Energy calculation function . . . 25

8 Acknowledgement **25**

1 Historical introduction

The study on analyzing the dynamics of ellipsoids has been essential to understand the rotational movement and behaviors of stars, planets, gas clouds, and galaxies. Newton, one of the very first scientists and mathematicians to study the figure of earth, showed that the earth is an oblate spheroid, i.e., its equatorial radius is larger than its polar axis, instead of a prolate spheroid, which is the opposite. After Newton, more and more mathematicians started to study the behaviors of different types of ellipsoids, including Maclaurin, Jacobi, Dirichlet, Dedekind, Riemann, etc., where most of them had certain type of ellipsoids named after their names.

In short, Maclaurin Spheroids are in the shape of oblate spheroids, which rotate with a constant angular velocity as a rigid body under the equilibrium. Jacobi Ellipsoids also rotate with a constant angular velocity as a rigid body, but they have three different lengths of principal axes. Then, Dedekind Ellipsoids have the similar shape as Jacobi Ellipsoids, but all the fluid particles inside the ellipsoid are moving in elliptic trajectories centered at the center of the ellipsoid; when the ellipsoid is at its equilibrium, it is not rotating, but all the fluid particles inside are. Riemann Ellipsoids are more complicated, where the fluid particles moves in circles that are not centered at the same center as that of the ellipsoid, and the ellipsoid itself is also rotating.

Notably, in 1969, Chandrasekhar [1] collected the studies of those mathematicians, solved, and showed the *Ellipsoidal Figures of Equilibrium* by using the virial equations. In 2009, Morrison, Lebovitz, and Biello [2] used Hamiltonian to describe the problem. Both studied the incompressible ellipsoid with gravity force to understand the problem, while some authors studied the compressible case or used surface tension. We shall look at the case discussed in Chandrasekhar [1] and Morrison et al. [2].

2 Mathematical background

2.1 Fluid dynamics

The equations for the Riemann ellipsoids arise from fluid dynamics, where we assume that the fluid inside the ellipsoids is incompressible ideal fluid, with gravity being the only body force. Therefore, the incompressible Euler equations, which satisfy all three conditions mentioned, are,

$$\frac{\partial \boldsymbol{u}}{\partial t} + \boldsymbol{u} \cdot \nabla \boldsymbol{u} = -\frac{\nabla p}{\rho} + \nabla \chi \tag{1}$$

$$\nabla \cdot \boldsymbol{u} = 0 \tag{2}$$

$$\frac{\partial \rho}{\partial t} + \boldsymbol{u} \cdot \nabla \rho = 0 \tag{3}$$

where $\boldsymbol{u} = \boldsymbol{u}(\boldsymbol{x}, t)$ denotes velocity field inside the ellipsoids, $p = p(\boldsymbol{x}, t)$ denotes the pressure in the normal direction, ρ denotes the density of the fluid inside the ellipsoids, and $\chi = -gz$ denotes the gravitational potential that applies to the entire body of the ellipsoids. And (1) is the momentum equation, (2) shows the incompressibility, and (3) is the mass conservation equation.

2.1.1 The derivation of the momentum equation

The Momentum Equation comes from Newton's Second Law, where the time rate of change of the momentum is equal to the net force:

$$\frac{d}{dt}\int_{\Omega(t)} \rho\, \boldsymbol{u}\, dV = \int_{\Omega(t)} \rho\, \boldsymbol{f}\, dV + \int_{\partial\Omega(t)} \boldsymbol{f}_s\, dA \tag{4}$$

where $\Omega(t)$ is the domain of the fluid, $\boldsymbol{f}$ is the body force exerted on the fluid, $\partial\Omega(t)$ is the boundary of the fluid, and $\boldsymbol{f}_s$ is the surface force/stress exerted on the fluid.

For the left-hand side of the equation, we want to put the time derivative inside the integral. Using Reynolds Transport Theorem, we get that

$$\frac{d}{dt}\int_{\Omega(t)} \rho\, \boldsymbol{u}\, dV = \int_{\Omega(t)} \rho \frac{d\boldsymbol{u}}{dt}\, dV = \int_{\Omega(t)} \rho \left(\frac{\partial \boldsymbol{u}}{\partial t} + \boldsymbol{u} \cdot \nabla \boldsymbol{u}\right) dV \tag{5}$$

For the second term of the right-hand-side equation, since we are dealing with ideal fluids, whose stress is an isotropic pressure in the normal direction, then there is no tangential stresses, no friction, and the size of the force does not depend on the orientation. Therefore, the surface force can be written as

$$\boldsymbol{f}_s = \sigma \cdot \boldsymbol{n} \tag{6}$$

where $\boldsymbol{n} = \boldsymbol{n}(\boldsymbol{x})$ with $\boldsymbol{x} \in \partial\Omega(t)$ is the normal vector of the boundary of the fluid, and

$$\sigma = \begin{pmatrix} -p & 0 & 0 \\ 0 & -p & 0 \\ 0 & 0 & -p \end{pmatrix} \tag{7}$$

Plugging it back into (4) and applying the divergence theorem, we get

$$\int_{\partial\Omega(t)} \boldsymbol{f}_s \, dA = \int_{\Omega(t)} \nabla \cdot \sigma \, dV = \int_{\Omega(t)} -\nabla p \, dV \tag{8}$$

Therefore, assuming the flow is smooth everywhere in the domain and the body force being the gravitational force only, we get (1), the momentum equation mentioned above.

2.1.2 Incompressibility

The incompressibility means that the volume of the fluid does not change as the time evolves, i.e.,

$$\frac{d}{dt} \int_{\Omega(t)} d\vec{x} = 0 \tag{9}$$

Changing the coordinates to the Lagrangian Coordinates, we have

$$\begin{aligned} \frac{d}{dt} \int_{\Omega(t)} d\vec{x} &= \int_{\Omega(0)} \frac{\partial}{\partial t} |J| \, d\vec{a} \\ &= \int_{\Omega(0)} \nabla \cdot \boldsymbol{u} \cdot |J| \, d\vec{a} \\ &= \int_{\Omega(t)} \nabla \cdot \boldsymbol{u} \, d\vec{x} \end{aligned} \tag{10}$$

where $J_{ij} = \frac{\partial x_i}{\partial a_j}$ and $\vec{a} = \vec{x}(0)$ is the Lagrangian Coordinate. Plugging (10) into (9), we get equation (2).

2.1.3 Mass conservation

To obtain the mass conservation equation, let Ω be a fixed domain, then

$$\frac{d}{dt} \int_{\Omega} \rho \, dV = - \int_{\partial\Omega} \rho \, \boldsymbol{u} \cdot \boldsymbol{n} \, dA \tag{11}$$

where the left-hand side denotes the time rate of change of the mass, and the right-hand side denotes the amount of fluid that's coming out or into the fluid. Since Ω is fixed and because of the divergence theorem, we have

$$\int_{\Omega} \frac{\partial \rho}{\partial t} \, dV = \int_{\Omega} \nabla \cdot (\rho \, \boldsymbol{u}) \, dV \tag{12}$$

Combining with the incompressibility equation, we get equation (3).

2.2 The ordinary differential equations (ODEs) describing the fluid ellipsoids

Now, according to Morrison et al. [2], who used Dirac brackets and Hamiltonian reduction to achieve the matrix equations, which are equivalent to the Euler equations, (1), (2), and (3), we mentioned above.

First, let us define the moment of inertia matrix Σ and the first moment of the velocity field matrix M that will be used in solving the dynamics of the ellipsoids. Let

$$\Sigma_{ij} = \int_{\Omega} \rho x_i x_j dV \tag{13}$$

which denotes the second order moment of the density field over Ω, the domain of the ellipsoid, where

$$\rho(\boldsymbol{x}, t) = \begin{cases} \rho_0 & \boldsymbol{x} \in \Omega \\ 0 & \text{otherwise} \end{cases} \tag{14}$$

where ρ_0 is a constant. And for the simplicity in the future, define

$$\hat{\Sigma}^{-1} = \frac{\Sigma^{-1}}{tr\left(\Sigma^{-1}\right)} \tag{15}$$

Then, let us define

$$M_{ij} = \int_\Omega \rho x_i u_j dV \tag{16}$$

which denotes the first order moment of momentum density field over the same domain, and we define the velocity to be a linear function of the coordinate, i.e., $\boldsymbol{u} = L \cdot \boldsymbol{x}$, where $L = L(t)$ is a square matrix, and we have

$$M_{ij} = \int_\Omega \rho x_i L_{jk} x_k \, dV = L_{jk} \int_\Omega \rho x_i x_k \, dV \tag{17}$$

$$= \Sigma_{ik} \cdot L_{jk} \tag{18}$$

I.e.

$$M = \Sigma \cdot L^T \tag{19}$$

After the applications of Dirac brackets and Hamiltonian reduction, Morrison et al. [2] showed that the time derivatives of Σ and M can be written in the form:

$$\dot{\Sigma}_{ij} = \{\Sigma_{ij}, M_{kl}\} \frac{\partial H}{\partial M_{kl}} + \{\Sigma_{ij}, \Sigma_{kl}\} \frac{\partial H}{\partial \Sigma_{kl}} \tag{20}$$

and

$$\dot{M}_{ij} = \{M_{ij}, M_{kl}\} \frac{\partial H}{\partial M_{kl}} + \{M_{ij}, \Sigma_{kl}\} \frac{\partial H}{\partial \Sigma_{kl}} + \{M_{ij}, \Sigma_{kl}\} \frac{\partial V}{\partial \Sigma_{kl}} \tag{21}$$

where H is the hamiltonian/kinetic energy of the system, V is the potential energy of the system, and the brackets are Dirac brackets that are derived by Morrison et al. [2], where

$$\begin{aligned}
\{M_{ij}, M_{kl}\} &= \delta_{ij} M_{kj} - \delta_{jk} M_{il} + \delta_{ij}\left(\hat{\Sigma}^{-1}_{kn} M_{nl} + \hat{\Sigma}^{-1}_{ln} M_{nk}\right) - \delta_{kl}\left(\hat{\Sigma}^{-1}_{in} M_{nj} + \hat{\Sigma}^{-1}_{jn} M_{ni}\right) \\
\{M_{ij}, \Sigma_{kl}\} &= \frac{2\delta_{ij}\delta_{kl}}{tr\left(\Sigma^{-1}\right)} - \left(\delta_{jk}\Sigma_{il} + \delta_{jl}\Sigma_{ik}\right) \\
\{\Sigma_{ij}, M_{kl}\} &= -\{M_{kl}, \Sigma_{ij}\} \\
\{\Sigma_{ij}, \Sigma_{kl}\} &= 0
\end{aligned} \tag{22}$$

2.2.1 The Hamiltonion/kinetic energy

H in equation (20) and (21) is the Hamiltonian and kinetic energy of the system, and we have

$$\begin{aligned}
H = \int_\Omega \rho \frac{\boldsymbol{u}^2}{2} \, dV &= \frac{\rho_0}{2} \int_\Omega u_i^2 \, dV \\
&= \frac{\rho_0}{2} \int_\Omega \left(L_{ij} {x_j}^2\right) \, dV \\
&= \frac{\rho_0}{2} \int_\Omega x_j L^T_{ji} L_{ij} x_j \, dV \\
&= \frac{1}{2} tr(L \Sigma L^T) \\
&= \frac{1}{2} tr(M^T \Sigma^{-1} M)
\end{aligned} \tag{23}$$

Then, from Morrison et al. [2], we have the gradients of H

$$\frac{\partial H}{\partial \Sigma} = -\frac{1}{2} \Sigma^{-1} M M^T \Sigma \tag{24}$$

and

$$\frac{\partial H}{\partial M} = \Sigma^{-1} M \tag{25}$$

2.2.2 Potential energy

By definition, the potential energy is

$$V = \int_\Omega \rho \, P \, dV \tag{26}$$

where P is the gravitational potential of the ellipsoids, which we get from Chandrasekhar [1]

$$P = \pi G \rho (I - \sum_{i=1}^{3} A_i x_i^2) \tag{27}$$

where

$$A_i = a_1 a_2 a_3 \int_0^\infty \frac{du}{\sqrt{(a_1^2+u)(a_2^2+u)(a_3^2+u)}} \cdot \frac{1}{(a_i^2+u)} \tag{28}$$

and

$$I\left(a_1, a_2, a_3\right) = a_1 a_2 a_3 \int_0^\infty \frac{du}{\sqrt{(a_1^2+u)(a_2^2+u)(a_3^2+u)}} \tag{29}$$

with a_i being the length of the principal axes of the ellipsoids. Plugging equation (27) into (26), we will get from Morrison et al. [2],

$$V = -k \frac{m}{5} I(a_1, a_2, a_3) \tag{30}$$

where $k = 2\pi G \rho_0$. Then, we will get

$$\frac{\partial V}{\partial \Sigma} = -\frac{k}{2} \frac{m}{5} \left(I \Sigma^{-1} - \frac{5}{m} \tilde{A} \right) \tag{31}$$

where $\tilde{A} = RAR^T$ with $A = diag(A_i)$ and R being the rotation matrix describing the rotation of the ellipsoids.

2.2.3 The ODEs of the systems

Then, by applying equation (22), (24), (25), and (31) to (20) and (21), we get from Morrison et al. [2], that

$$\dot{\Sigma} = M + M^T - 2I \cdot tr\left(\hat{\Sigma}^{-1} M\right) \tag{32}$$

and

$$\dot{M} = M^T \Sigma^{-1} M + I \cdot tr\left(\hat{\Sigma}^{-1} M \Sigma^{-1} M\right) - tr\left(\hat{\Sigma}^{-1} M\right) \cdot \left(\Sigma^{-1} M + M^T \Sigma^{-1}\right) + k \left[\frac{2I}{Tr[\Sigma^{-1}]} - \Sigma \tilde{A}\right] \tag{33}$$

Notice that since $M = \Sigma L^T$, we have $tr\left(\hat{\Sigma}^{-1} M\right) = \frac{tr(L)}{tr\left(\Sigma^{-1}\right)}$.

3 Conserved quantities

Now, we shall discuss the conserved quantities in the system because we can understand the system better, get a simpler form of the ODEs, and check the validity of the codes when visualizing the rotations of the ellipsoids.

3.1 Total energy

Total energy is also a quantity that should always be conserved. In our case, the total energy E is the sum of kenetic energy and potential energy, therefore

$$E = H + V \tag{34}$$

where H is the kinetic energy defined in (23), and V is the potential energy defined in (30) that arises from the gravitational force. Therefore, the total energy

$$E = \frac{1}{2} tr(M^T \Sigma^{-1} M) - k \frac{m}{5} I(a_1, a_2, a_3) \tag{35}$$

should be conserved.

3.2 Kelvin's circulation

From Kelvin's Circulation Theorem, the circulation of a barotropic ideal fluid with conservative body force over a simple, closed curve does not change over time, i.e.

$$\frac{d}{dt}\oint_{\boldsymbol{c}} \boldsymbol{u} \cdot d\boldsymbol{s} = 0 \tag{36}$$

From Rosensteel [4], we can get the circulation from the matrix form

$$\Gamma^2 = tr\left(\Sigma^{-1} M \Sigma M^T - MM\right) \tag{37}$$

which should be conserved in the system.

3.3 Total volume

According to the assumption of incompressibility, which means the rate of change of volume with respect to time is zero, we should get a constant volume for the ellipsoids for all time, t.

Let D be the matrix that describes a stationary ellipsoid with principal axes a_1, a_2, and a_3, and R be the rotation matrix that describes the rotation of the ellipsoid. Then, we have

$$\Sigma = RDR^T \tag{38}$$

and

$$D_{ij} = \int_\Omega \left(\rho_0 \cdot x_i x_j\right)\, dx_1\, dx_2\, dx_3 \tag{39}$$

Let $x_i = a_i u_i$, we get

$$\int_\Omega \left(\rho_0 \cdot x_i x_j\right)\, dx_1\, dx_2\, dx_3 = \rho_0 a_1 a_2 a_3 \cdot a_i a_j \iiint \left(u_i u_j\right)\, du_1\, du_2\, du_3 \tag{40}$$

Then, transforming it into the spherical coordinates, we have

$$D_{ij} = \begin{cases} \frac{m}{5} a_i^2 & i = j \\ 0 & i \neq j \end{cases} \tag{41}$$

where $m = \rho_0 \cdot \frac{4}{3}\pi a_1 a_2 a_3$ is the mass of the ellipsoid. Notice that D is a diagonal matrix, hence $D^T = D$ and $\Sigma^T = \Sigma$.

Then, to obtain the conservation of volume in matrix form, we just need to look at the determinant of Σ, since

$$det(\Sigma) = det(RDR^T) = det(D) \propto V^2 \tag{42}$$

3.4 Divergence of the velocity field

Similarly, because of the assumption of incompressibility, we have the divergence of the velocity field to be zero

$$\nabla \cdot \boldsymbol{u} = 0 \tag{43}$$

Using Einstein's notation, we can derive the divergence in the matrix form:

$$\begin{aligned} \nabla \cdot \boldsymbol{u} = \frac{\partial u_i}{\partial x_i} &= \frac{\partial}{\partial x_i}\left(L_{ij} x_j\right) \\ &= \frac{\partial L_{ij}}{\partial x_i} x_j + L_{ij}\frac{\partial x_j}{\partial x_i} \\ &= L_{ii} \end{aligned} \tag{44}$$

Therefore, we have

$$\nabla \cdot \boldsymbol{u} = tr(L) \tag{45}$$

Notice that since $tr(L) = tr(L^T) = tr(\Sigma^{-1} M)$, we can simplify equation (32) and (33) to

$$\dot{\Sigma} = M + M^T \tag{46}$$

and

$$\dot{M} = M^T \Sigma^{-1} M + I\frac{Tr[M^T \Sigma^{-1} M^T \Sigma^{-1}]}{Tr[\Sigma^{-1}]} + k\left[\frac{2I}{Tr[\Sigma^{-1}]} - \Sigma\tilde{A}\right] \tag{47}$$

4 The equilibrium solutions

In order to solve for the equilibrium solutions analytically, we shall understand the equilibrium conditions of different types of ellipsoids, and then transform the frame of reference from the inertial frame, which (46) and (47) are in.

4.1 The geometry of different types of ellipsoids

We are going to take a look at four main types of the ellipsoids. To understand the geometry, let us set the the ellipsoids on Cartesian Coordinates, where the ellipsoids center at the origin and with three principal axes, $\hat{a}_1$, $\hat{a}_2$, and $\hat{a}_3$, parallel to x-axis, y-axis, and z-axis. And let $a_1 \geq a_2 \geq a_3$.

In order to understand the motion of the ellipsoids under equilibrium, we shall use Roberts and Sousa Dias's method [3]. Let us define a function

$$\boldsymbol{x}(t) = T(t)\,\boldsymbol{x}_0 \tag{48}$$

where

$$T = R_2^T A_0 R_1 \tag{49}$$

with

$$A_0 = \begin{pmatrix} a_1 & 0 & 0 \\ 0 & a_2 & 0 \\ 0 & 0 & a_3 \end{pmatrix} \tag{50}$$

$$R_1 = \begin{pmatrix} \cos(\omega_1 t) & \sin(\omega_1 t) & 0 \\ -\sin(\omega_1 t) & \cos(\omega_1 t) & 0 \\ 0 & 0 & 1 \end{pmatrix} \tag{51}$$

$$R_2 = \begin{pmatrix} \cos(\omega_2 t) & \sin(\omega_2 t) & 0 \\ -\sin(\omega_2 t) & \cos(\omega_2 t) & 0 \\ 0 & 0 & 1 \end{pmatrix} \tag{52}$$

and $\boldsymbol{x}_0$ denotes all the points inside a unit sphere centered at the origin. Notice that we assume the ellipsoids are always rotating along the the shortest principal axis, i.e., the z-axis, hence the form of two rotation matrices above.

4.1.1 Maclaurin spheroids

For Maclaurin Spheroids, we have $a_1 = a_2 > a_3$ and $R_1 = I$. I.e., the spheres transform into oblate spheroids, then rotate in an angular velocity, ω_2, as rigid body. Then, we have

$$\boldsymbol{x} = \begin{pmatrix} \cos(\omega t) \\ \sin(\omega t) \\ z_0 \end{pmatrix} \tag{53}$$

where $\boldsymbol{x}$ is the trajectories of the fluid particles. Therefore, from $\boldsymbol{u} = L \cdot \boldsymbol{x}$, we have matrix L being a simple anti-symmetric matrix:

$$L = \begin{pmatrix} 0 & -\omega & 0 \\ \omega & 0 & 0 \\ 0 & 0 & 0 \end{pmatrix} \tag{54}$$

Figure 1 briefly shows the dynamics inside Maclaurin Spheroids:

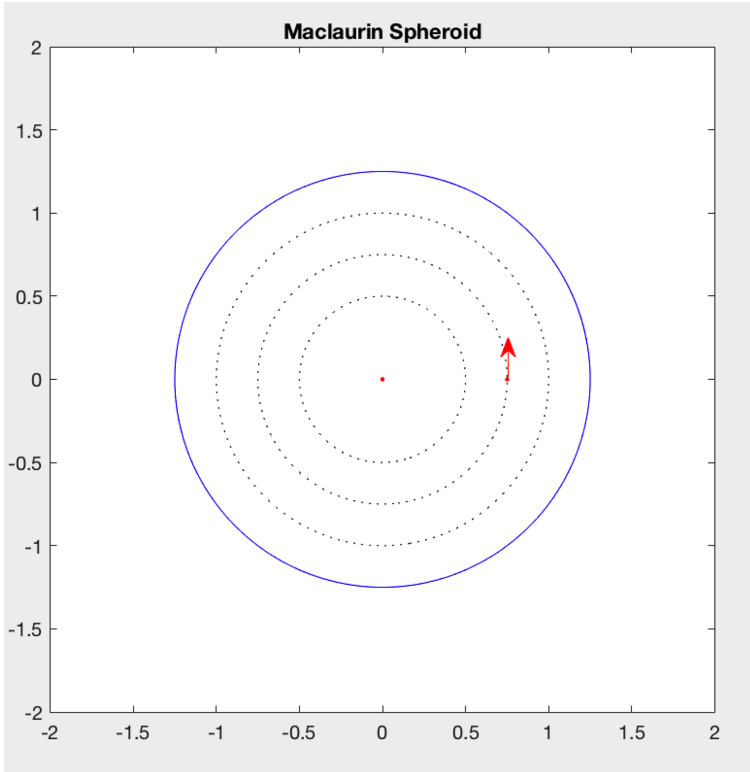

Figure 1: Maclaurin Spheroids

which is the horizontal cross-section of the spheroids. The dotted, concentric circles indicate the trajectories of the fluid particles, and they all move in the same angular velocity.

4.1.2 Jacobi ellipsoids

For Jacobi Ellipsoids, we have $a_1 > a_2 > a_3$ and $R_1 = I$. I.e., the spheres transform into ellipsoids, then, like Maclaurin Spheroids, rotate in an angular velocity, ω_2, as rigid body. Therefore, matrix L can be written in the same form as that of the Maclaurin Spheroids.

Figure 2 briefly shows the dynamics inside Jacobi Ellipsoids:

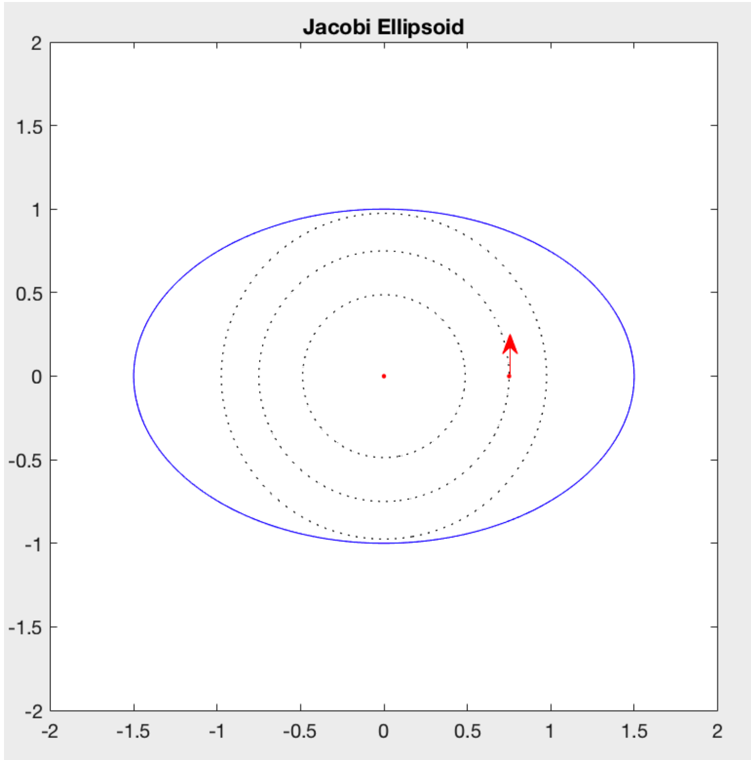

Figure 2: Jacobi Ellipsoids

which is the horizontal cross-section of the Ellipsoids. Just like the Maclaurin Spheroids, the dotted, concentric circles indicate the trajectories of the fluid particles, and they all move in the same angular velocity. However, we can also tell that the ellipsoids are rotating.

4.1.3 Dedekind ellipsoids

For Dedekind Ellipsoids, we also have $a_1 > a_2 > a_3$, but this time, $R_2 = I$. So all the fluid particles in the spheres start to rotate in an angular velocity, ω_1, then we transform the spheres into ellipsoids. Therefore, under the equilibrium, the ellipsoids as a complete object is not rotating, but all the fluid particles are moving in the concentric-ellipse trajectories centered at the origin. Then, we have

$$\boldsymbol{x} = \begin{pmatrix} a_1 \cdot r \cdot \cos(\omega t) \\ a_2 \cdot r \cdot \sin(\omega t) \\ z_0 \end{pmatrix} \tag{55}$$

where r is a positive constant. Therefore, from $\boldsymbol{u} = L \cdot \boldsymbol{x}$, we have

$$L = \begin{pmatrix} 0 & -\frac{a_1}{a_2} \cdot \omega & 0 \\ \frac{a_2}{a_1} \cdot \omega & 0 & 0 \\ 0 & 0 & 0 \end{pmatrix} \tag{56}$$

Figure 3 briefly shows the dynamics inside Dedekind Ellipsoids:

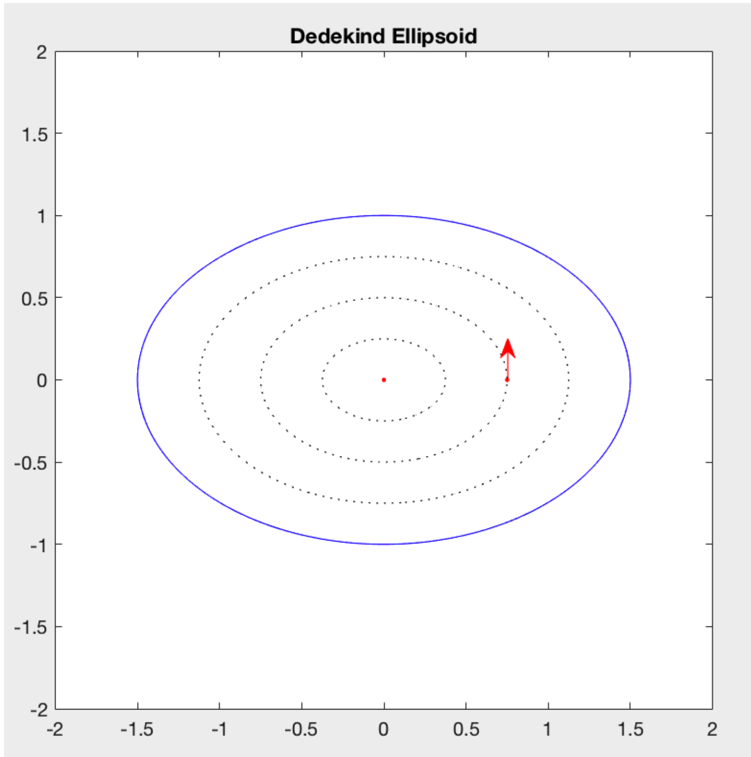

Figure 3: Dedekind Ellipsoids

which is the horizontal cross-section of the ellipsoids. The dotted, concentric ellipses indicate the trajectories of the fluid particles. We can not observe anything from the outside of the ellipsoids, but all the particles are moving in ellipses.

4.1.4 Riemann ellipsoids

For Riemann Ellipsoids, which are more complicated then the previous ones, we have $a_1 > a_2 > a_3$, and neither rotation matrices are identity matrix. In this case, we will have fluid particles moving in circles that are not centered at the origin, or ellipsoids not rotating along the z-axis. Because of the complexity, we shall not go into details about Riemann Ellipsoids in this paper.

4.2 Equilibrium solutions

4.2.1 Set-up

Recall that for Maclaurin Spheroids, $a_1 = a_2 > a_3$, and for Jacobi and Dedekind Ellipsoids, $a_1 > a_2 > a_3$, all ellipsoids rotate along z-axis and have matrix L, where

$$L = \begin{pmatrix} 0 & -\omega & 0 \\ \omega & 0 & 0 \\ 0 & 0 & 0 \end{pmatrix} \tag{57}$$

for Maclaurin Spheroids and Jacobi Ellipsoids, and

$$L = \begin{pmatrix} 0 & -\frac{a_1}{a_2} \cdot \omega & 0 \\ \frac{a_2}{a_1} \cdot \omega & 0 & 0 \\ 0 & 0 & 0 \end{pmatrix} \tag{58}$$

for Dedekind Ellipsoids, with

$$M = \Sigma \cdot L^T \tag{59}$$

and rotation matrix R, where

$$R = \begin{pmatrix} \cos(\omega t) & \sin(\omega t) & 0 \\ -\sin(\omega t) & \cos(\omega t) & 0 \\ 0 & 0 & 1 \end{pmatrix} \tag{60}$$

for Maclaurin Spheroids and Jacobi Ellipsoids, and $R = I$ for Dedekind Ellipsoids.

4.2.2 Changing to the rotational frame of reference

Since (46) and (47) are in initial frame and therefore complicated, we shall rewrite the equation in a simpler form with the rotating frame of reference.

Let N be the matrix of M before the rotation, D be the matrix of Σ before the rotation as defined in (41), and K be the matrix of L before the rotation. Therefore, we have

$$M = RNR^T \tag{61}$$

$$\Sigma = RDR^T \tag{62}$$

$$L = RKR^T \tag{63}$$

Also, let us define angular velocity matrix Ω as:

$$\Omega = \dot{R}^T R \tag{64}$$

Notice that,

$$\Omega^T = R^T \dot{R} \tag{65}$$

Then we will have,

$$\Omega + \Omega^T = \frac{d}{dt}\left(R^T R\right) = \frac{dI}{dt} = 0 \tag{66}$$

which implies that Ω is an asymmetric matrix.

Now, plugging (61), (62), and (63) into (46) and (47), and multiplying each term in by R^T on left side and R on right side, we get

$$R^T \dot{R} D + \dot{D} + D\dot{R}^T R = N + N^T \tag{67}$$

and

$$R^T \dot{R} N + \dot{N} + N\dot{R}^T R = N^T D^{-1} N + I\frac{Tr[L^2]}{Tr[D^{-1}]} + k\left[\frac{2I}{Tr[D^{-1}]} - DA\right] \tag{68}$$

Plugging (64), (65), and (66) in, we get

$$\dot{D} + D\Omega - \Omega D = N + N^T \tag{69}$$

and

$$\dot{N} + N\Omega - \Omega N = N^T D^{-1} N + I\frac{Tr[L^2]}{Tr[D^{-1}]} + k\left[\frac{2I}{Tr[D^{-1}]} - DA\right] \tag{70}$$

To get a simpler form, we want to write N in the form of D and K. Notice that (58), (61), (62), and (63) give us:

$$N = DK^T \tag{71}$$

and since R is orthogonal, $tr\left(R^T AR\right) = tr(A)$ for any matrix A.
Now, plug (71) into (69) and (70), we get:

$$\dot{D} = \Omega D - D\Omega + DK^T + KD \tag{72}$$

and

$$K\dot{D} + \dot{K}D - \Omega KD + KD\Omega - KDK^T = I\frac{Tr[K^2]}{Tr[D^{-1}]} + k\left[\frac{2I}{Tr[D^{-1}]} - AD\right] \tag{73}$$

Then plug in (72) and multiply each term on the right side by D^{-1}, we get

$$K^2 + \dot{K} + K\Omega - \Omega K = D^{-1}\frac{Tr[K^2]}{Tr[D^{-1}]} + k\left[\frac{2D^{-1}}{Tr[D^{-1}]} - A\right] \tag{74}$$

4.2.3 Equilibrium solutions for Maclaurin spheroids and Jacobi ellipsoids

For Maclaurin Spheroids and Jacobi Ellipsoids, we get L from equation (57) and $K = L$. And one can show that $K\Omega - \Omega K = 0$. Setting $\dot{K} = 0$, we have

$$\begin{pmatrix} -\omega^2 & 0 & 0 \\ 0 & -\omega^2 & 0 \\ 0 & 0 & 0 \end{pmatrix} = \frac{2k - 2\omega^2}{\frac{1}{a_1^2} + \frac{1}{a_2^2} + \frac{1}{a_3^2}} \begin{pmatrix} \frac{1}{a_1^2} & 0 & 0 \\ 0 & \frac{1}{a_2^2} & 0 \\ 0 & 0 & \frac{1}{a_3^2} \end{pmatrix} - k \begin{pmatrix} A_1 & 0 & 0 \\ 0 & A_2 & 0 \\ 0 & 0 & A_3 \end{pmatrix} \tag{75}$$

which implies

$$\begin{aligned} &\left(\frac{1}{a_1^2} + \frac{1}{a_2^2} + \frac{1}{a_3^2}\right) \begin{pmatrix} \omega^2 & 0 & 0 \\ 0 & \omega^2 & 0 \\ 0 & 0 & 0 \end{pmatrix} - \begin{pmatrix} \frac{2\omega^2}{a_1^2} & 0 & 0 \\ 0 & \frac{2\omega^2}{a_2^2} & 0 \\ 0 & 0 & \frac{2\omega^2}{a_3^2} \end{pmatrix} \\ &= k \left[\left(\frac{1}{a_1^2} + \frac{1}{a_2^2} + \frac{1}{a_3^2}\right) \begin{pmatrix} A_1 & 0 & 0 \\ 0 & A_2 & 0 \\ 0 & 0 & A_3 \end{pmatrix} - \begin{pmatrix} \frac{2}{a_1^2} & 0 & 0 \\ 0 & \frac{2}{a_2^2} & 0 \\ 0 & 0 & \frac{2}{a_3^2} \end{pmatrix} \right] \end{aligned} \tag{76}$$

Hence, calculating entry (1,1), (2,2), and (3,3) gives us:

$$\left(\frac{1}{a_2^2} + \frac{1}{a_3^2} - \frac{1}{a_1^2}\right)\omega^2 = k\left[(A_1 - 2)\frac{1}{a_1^2} + A_1\left(\frac{1}{a_2^2} + \frac{1}{a_3^2}\right)\right] \tag{77}$$

$$\left(\frac{1}{a_1^2} + \frac{1}{a_3^2} - \frac{1}{a_2^2}\right)\omega^2 = k\left[(A_2 - 2)\frac{1}{a_2^2} + A_2\left(\frac{1}{a_1^2} + \frac{1}{a_3^2}\right)\right] \tag{78}$$

$$-\frac{2\omega^2}{a_3^2} = k\left[(A_3 - 2)\frac{1}{a_3^2} + A_3\left(\frac{1}{a_2^2} + \frac{1}{a_1^2}\right)\right] \tag{79}$$

Notice that if we add these three equations, we will get $A_1 + A_2 + A_3 = 2$, which is what we expect, and since we know how to get A_i, these three equations are actually equivalent.

- For Maclaurin Spheroids, we require $a_1 = a_2 > a_3$, therefore, by Chandrasekhar [1], we have $A_1 = A_2$. Plug them and $A_1 + A_2 + A_3 = 2$ in any one of (77), (78), or (79), we can get:

  $$\omega^2 = k\left[\left(-\frac{1}{2}\right)(-2A_1) - \left(\frac{A_3}{2}\right)\left(\frac{2}{a_1^2}\right)a_3^2\right] \tag{80}$$

  Therefore, we reach to the final solution. Maclaurin Spheroid is under equilibrium when the relation between its vorticity, ω, and eccentricity, $e = \left(1 - \frac{a_3^2}{a_1^2}\right)^{\frac{1}{2}}$, satisfies the following equation:

  $$\frac{\omega^2}{\pi G \rho_0} = 2\left(A_1 - \frac{a_3^2}{a_1^2}A_3\right) \tag{81}$$

  where $A_1 = \frac{(1-e^2)^{\frac{1}{2}}}{e^3}\sin^{-1}(e) - \frac{1-e^2}{e^2}$ and $A_3 = 2 - 2A_1$.

- For Jacobi Ellipsoid, since the length of each principal axis is different, where $a_1 > a_2 > a_3$, we will obtain different values for A_1, A_2, and A_3. Since it still satisfies that $A_1 + A_2 + A_3 = 2$, we can get the value of ω^2 using the same equation, (81), with the values of A_1 and A_3 calculated by Chandrasekhar [1] being:

  $$A_1 = \frac{2a_2a_3}{a_1^2 \sin^3(\phi)\sin^2(\theta)}[F(\theta,\phi) - E(\theta,\phi)] \tag{82}$$

  $$A_3 = \frac{2a_2a_3}{a_1^2 \sin^3(\phi)\cos^2(\theta)}\left[\frac{a_2}{a_3}\sin(\phi) - E(\theta,\phi)\right] \tag{83}$$

where

$$E(\theta,\phi) = \int_0^{\phi} \left(1 - \sin^2(\theta)\sin^2(\phi)\right)^{\frac{1}{2}} d\phi \tag{84}$$

$$F(\theta,\phi) = \int_0^{\phi} \left(1 - \sin^2(\theta)\sin^2(\phi)\right)^{-\frac{1}{2}} d\phi \tag{85}$$

with $\sin(\theta) = \left(\frac{a_1^2 - a_2^2}{a_1^2 - a_3^2}\right)^{\frac{1}{2}}$ and $\cos(\phi) = \frac{a_3}{a_1}$.

4.2.4 Equilibrium solutions for Dedekind ellipsoids

For Dedekind ellipsoids, since the ellipsoids are not rotating under the equilibrium, we have $R = I$, $\Omega = 0$, and $K = L$. Therefore, from equation (74), and setting $\dot{K} = 0$, we get:

$$L^2 = D^{-1}\frac{Tr[L^2]}{Tr[D^{-1}]} + k\left[\frac{2D^{-1}}{Tr[D^{-1}]} - A\right] \tag{86}$$

where

$$L = \begin{pmatrix} 0 & -\frac{a_1}{a_2}\cdot\omega & 0 \\ \frac{a_2}{a_1}\cdot\omega & 0 & 0 \\ 0 & 0 & 0 \end{pmatrix} \tag{87}$$

Then, plugging L into (86), we get

$$\begin{pmatrix} -\omega^2 & 0 & 0 \\ 0 & -\omega^2 & 0 \\ 0 & 0 & 0 \end{pmatrix} = \frac{2k - 2\omega^2}{\frac{1}{a_1^2} + \frac{1}{a_2^2} + \frac{1}{a_3^2}} \begin{pmatrix} \frac{1}{a_1^2} & 0 & 0 \\ 0 & \frac{1}{a_2^2} & 0 \\ 0 & 0 & \frac{1}{a_3^2} \end{pmatrix} - k \begin{pmatrix} A_1 & 0 & 0 \\ 0 & A_2 & 0 \\ 0 & 0 & A_3 \end{pmatrix} \tag{88}$$

which is exactly the same as equation (75). Therefore, since Dedekind Ellipsoids have the same condition for their principal axes as that of Jacobi Ellipsoids', where $a_1 > a_2 > a_3$, Dedekind Ellipsoids have the same equilibrium solution sets as Jacobi Ellipsoids do, which have been calculated and shown in equation (81) with the conditions (82)-(85).

5 Visualization of the ellipsoids and conserved quantities

In order to visualize our results from the equilibrium solutions, we constructed some codes on MatLab. And there are some interesting graphs.

5.1 Conserved quantities

We already derived four conserved quantities in the previous section, and now we shall use them to check the validity of our codes.

1. Total energy: Using equation (35), we get the total energy, and Figure 4 shows that the total energy is in fact conserved, since the error is less than $4 \cdot 10^{-9}$.

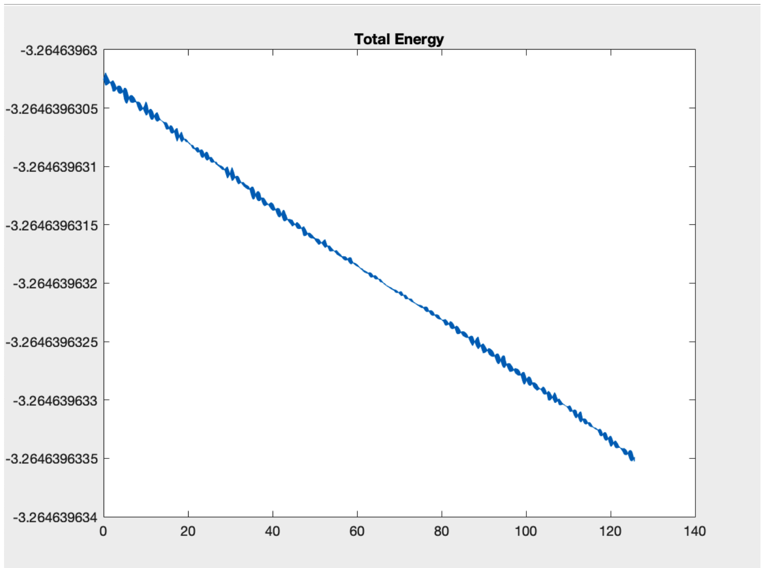

Figure 4: Total Energy

2. Kelvin's circulation: Using equation (37), we get Kelvin's circulation. Figure 5 shows that the Kelvin's circulation is also conserved in the system, since the error is less than $6 \cdot 10^{-10}$.

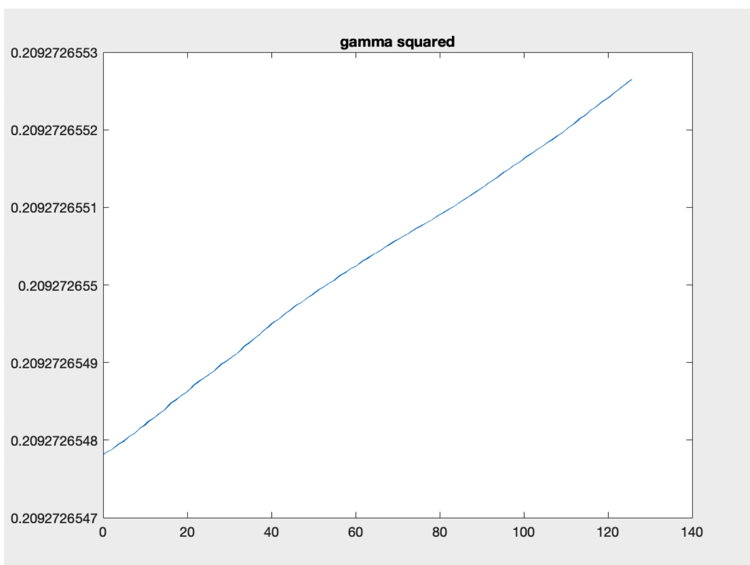

Figure 5: Γ^2

3. Total volume: Using equation (42), we get the total volume. Figure 6 below shows the total volume from our codes, which is conserved, since the error is less than $3 \cdot 10^{-9}$.

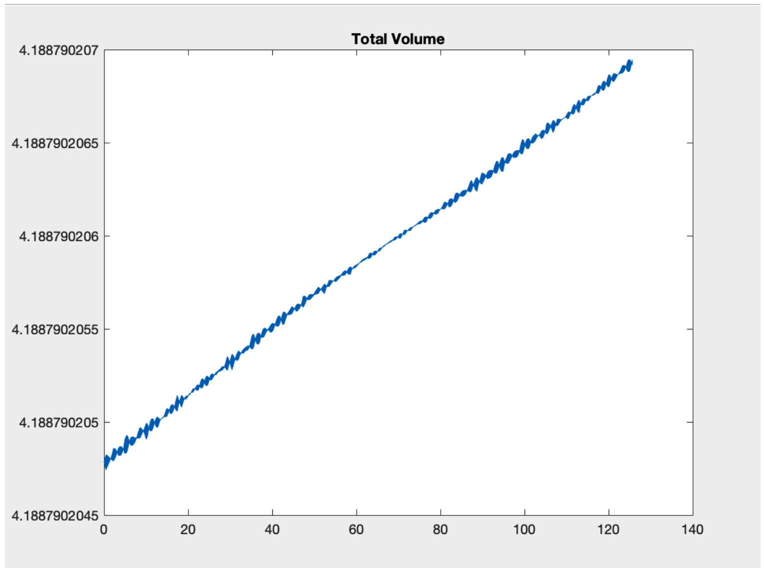

Figure 6: Total Volume

4. Divergence of the velocity field: Using equation (45), we get the divergence of the velocity field. Figure 7 below shows the conservation of the divergence of the velocity field, where the error is less than $7 \cdot 10^{-11}$.

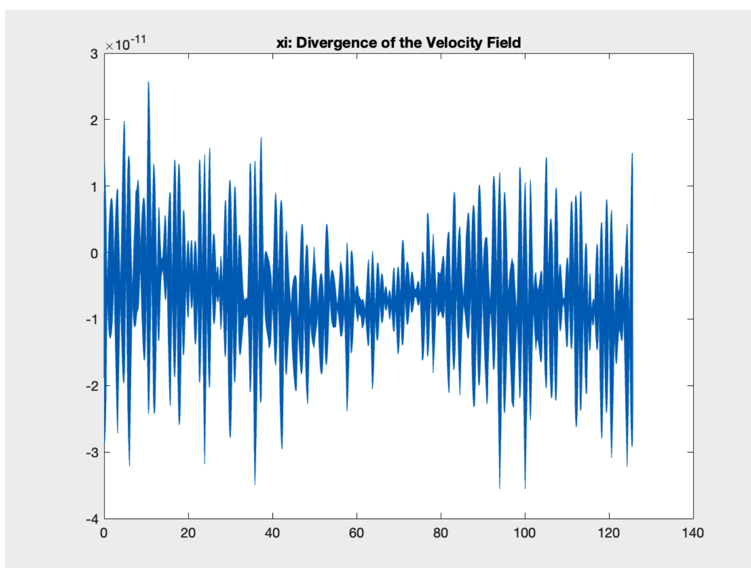

Figure 7: Divergence of the Velocity Field

Therefore, the codes work for those conserved quantities.

5.2 Equilibrium of the Maclaurin Spheroid and its dynamics near the equilibrium state

Using the results we got in §4.2.3, we can see that the Maclaurin Spheroid is under the equilibrium. In Figure 8, it is when $e = 0.98$, with green line indicating a_1 and a_2 and blue line indicationg a_3, and this will be same for all the Maclaurin Spheroid Figures.

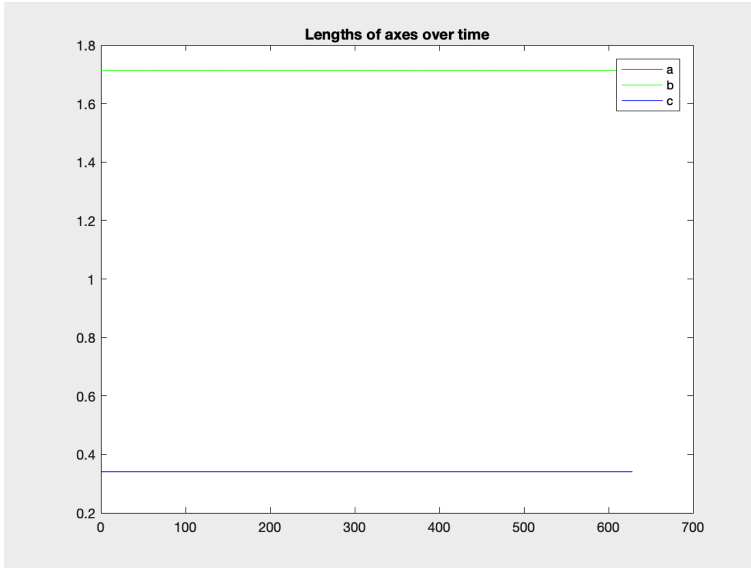

Figure 8: Maclaurin Spheroids under equilibrium

Then, if we let $a_1|_{t=0} = C = 1.01 \cdot a_1^*$, where a_1^* is the equilibrium solution we obtained, we will get Figure 9. And the spheroid seems to be on a periodic orbit.

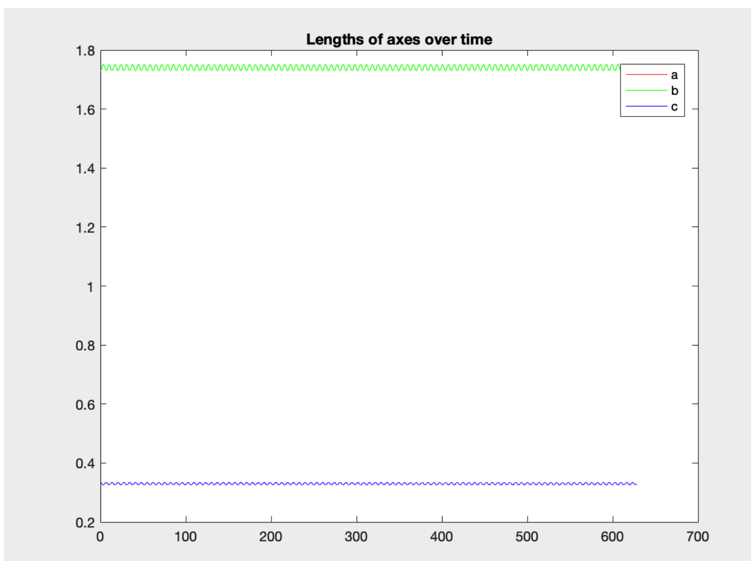

Figure 9: Maclaurin Spheroids under perturbation: C = 1.01

If we let $a_1|_{t=0} = C = 1.1 \cdot a_1^*$, we will get Figure 10. And the spheroid seems to be on a periodic orbit, too.

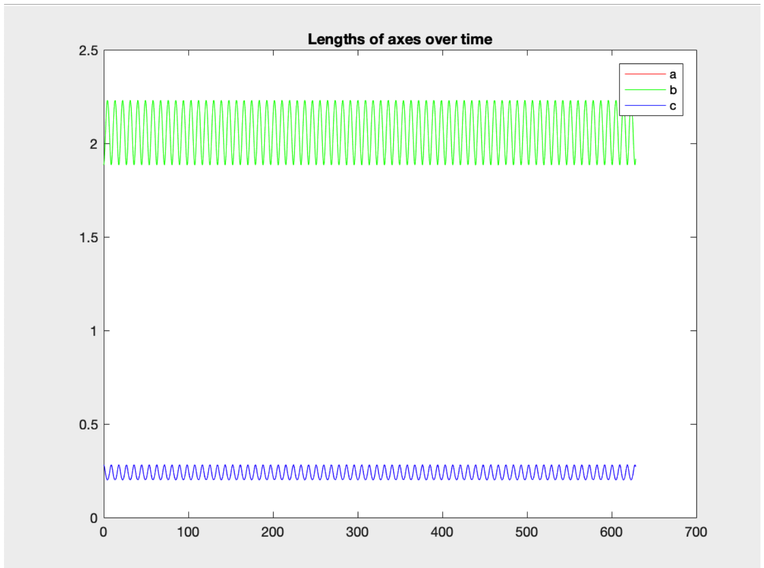

Figure 10: Maclaurin Spheroids under perturbation: C = 1.1

Then, if we let $a_1|_{t=0} = C = 1.4 \cdot a_1^*$, we will get Figure 11. Even though the lengths of axes are still periodic, but the derivatives are not continuous anymore.

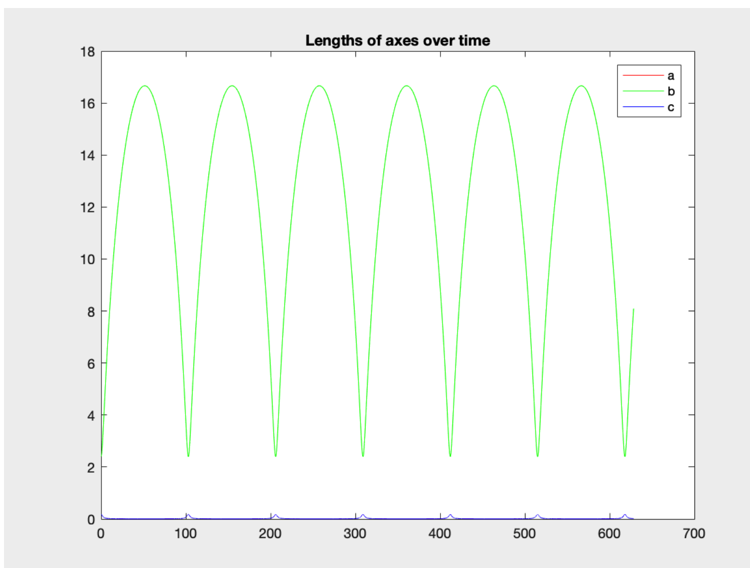

Figure 11: Maclaurin Spheroids under perturbation: C = 1.4

Now, if we let $a_1|_{t=0} = C = 1.5 \cdot a_1^*$, the spheroid finally blows up, as shown in Figure 12

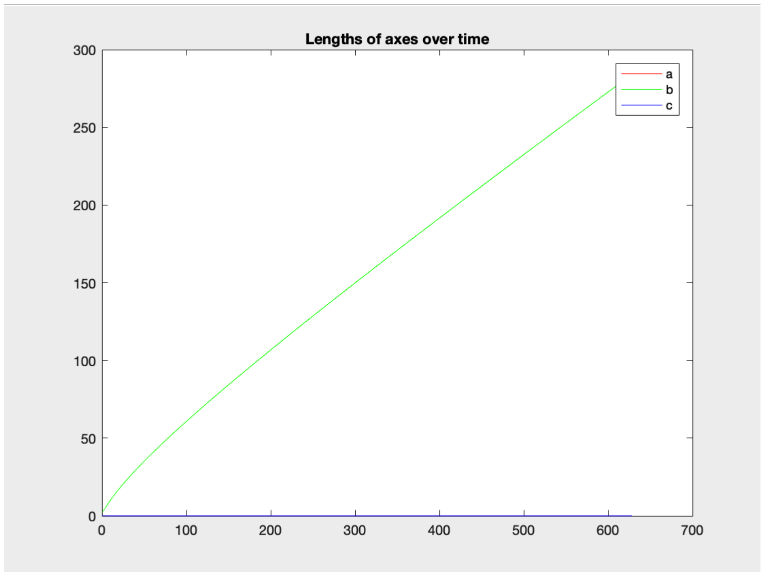

Figure 12: Maclaurin Spheroids under perturbation: C = 1.5

5.3 Equilibrium of the Jacobi Ellipsoid and its dynamics near the equilibrium state

Like Maclaurin Spheroid, Jacobi Ellipsoid also behaves in a similar way. Using the results in §4.2.3, we get Figure 13, which shows the lengths of axes of the Jacobi Ellipsoid under the equilibrium, where the ratio of three axes is $1 : 0.52 : 0.393944$. The red line indicates a_1, the green line indicates a_2, and the blue line indicates a_3

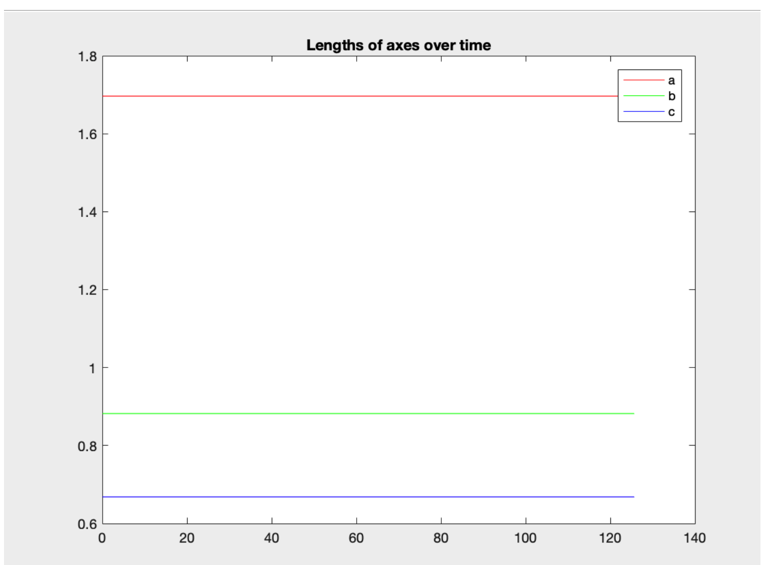

Figure 13: Jacobi Ellipsoid under equilibrium

Then, if we let $a_1|_{t=0} = C = 1.11 \cdot a_1^*$, where a_1^* is the equilibrium solution we obtained, we will get Figure 14. And the ellipsoid seems to be on a periodic orbit.

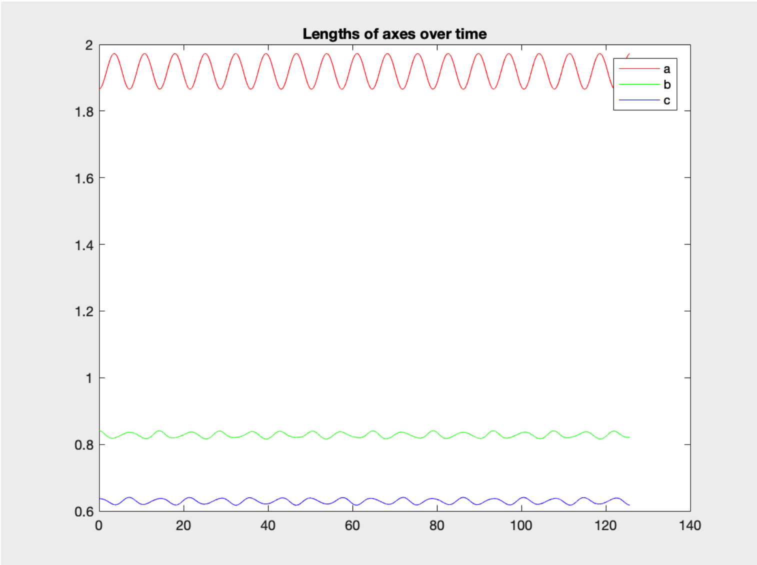

Figure 14: Jacobi Ellipsoid under perturbation: C = 1.11

However, if we let $a_1|_{t=0} = C = 1.5$, Figure 15 shows that, even though a_1 still appears to be periodic, a_2 and a_3 start to become unstable.

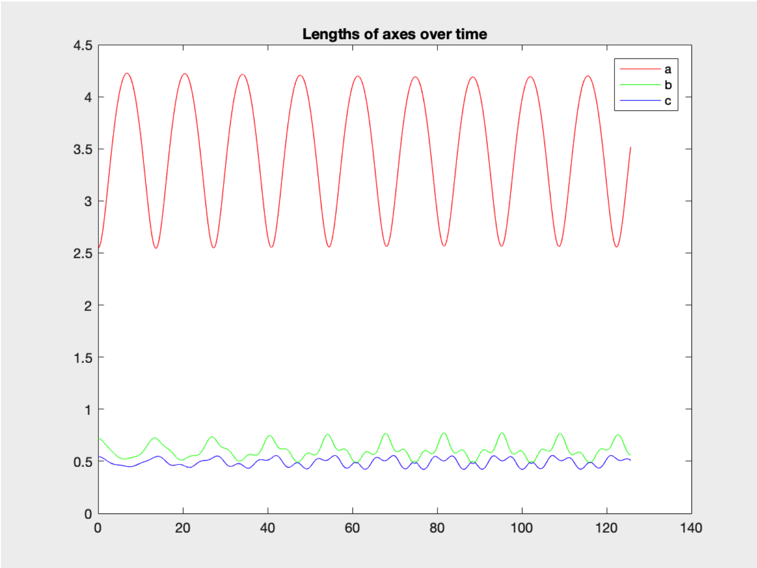

Figure 15: Jacobi Ellipsoid under perturbation: C = 1.5

Then, if we set $a_1|_{t=0} = C = 2.5$, we will get another blow-up, as shown in Figure 16

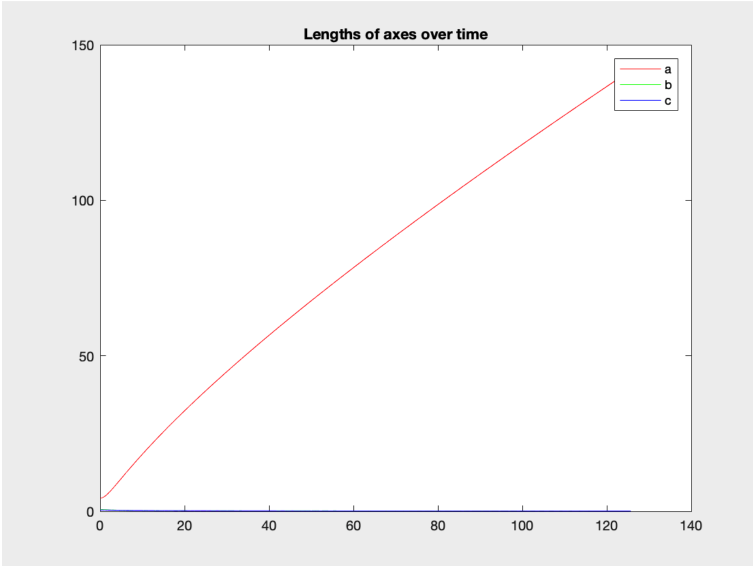

Figure 16: Jacobi Ellipsoid under perturbation: C = 2.5

6 Future work

We have figured out the equilibrium solutions for Maclaurin Spheroids, Jacobi Ellipsoids, and Dedekind Ellipsoids. However, for the latter two, we have not understood why they have the same equilibrium solutions and what makes the same solutions show completely different dynamical movements. So understanding that will be one thing we should do in the future. Also, the behaviors of Maclaurin Spheroids and Jacobi Ellipsoids in §5 are very similar to the solutions near a limit cycle, so we shall also take a look into that. And, because of the complexity of the dynamics of Riemann Ellipsoids, we have not yet derived a solution for them, which should be another thing to look at.

7 Appendix

7.1 Main code

```
%% Make Data: Arbitrary Ellipsoids
% Set some parameters and do basic integration
% input initial conditions (change)
tic
tspan = [0 20*2*pi]; %set timespan

a = 1.2; %set axes
b = 1;
c = 1/(a*b);

alpha = 0; %set velocity matric
beta = 0;
w1 = 0.1;
w2 = 0.1;
w3 = 0.2;

%% other misc constants
L = [alpha  w3     -w2;
     -w3    beta    w1;
     w2     -w1    -(alpha+beta)];

rho = 1;
```

```
G = 1/(pi*rho);
fc = 1;

volume = 4/3*a*b*c*pi;

theta = 0;  % can choose 0 w/o l.o.g.
phi =  0; % can choose 0 w/o l.o.g.

D = [1/a^2 0 0 ; 0 1/b^2 0 ; 0 0 1/c^2];
R = [cos(theta)*cos(phi) -sin(theta) -cos(theta)*sin(phi); ...
    sin(theta)*cos(phi) cos(theta) -sin(theta)*sin(phi); sin(phi) ...
    0 cos(phi)]; %rotation matrix

sigma = rho/5*volume*R*D^(-1)*R';
M = sigma*transpose(L);
sigmainv = inv(sigma);
invsigmahat = (sigmainv/trace(sigmainv));

%initial conditions for ode45
y0 = matrixToVector(sigma,M);

%integrate
options = odeset('RelTol',1e-12,'AbsTol',1e-10);
[t,y] = ode45(@(t,y)riemann(t,y,G,rho,volume), tspan, y0, options);

filename = "a=" + string(a) + "_b=" + string(b) + "_c=" + string(c) + "_w1=" ...
    + string(w1) + "_w2=" + string(w2) + "_w3=" + string(w3)+ ".mat";
save(filename, 't', 'y')

% %% LOAD DATA
% load('a=0.75_b=0.75_c=1.7778_w1=0_w2=0_w3=0.5.mat','t','y')
% set variables for later use
size_y = size(y);
length_y = size_y(1,1);

%graph y (M and sigma)
figure(fc)
fc = fc + 1;
plot(y)
title('y')

%make M and sigma from y (at each timestep)
[Mf, sigmaf] = vectorToMatrixCell(y);

%return rotation matrix and axes (at each timestep)
[Rf, at, bt, ct] = get_axes(length_y, sigmaf, rho);

%% Total Volume
%calculate and graph volume
[Vol, fc] = volume_calc(length_y,t,at,bt,ct,fc);

%% plot axes
fc = plot_axes(t,at,bt,ct,fc);

%% Gamma_squared
%calculate and graph gamma_squared
fc = gamma_calc(length_y,t, Mf, sigmaf, fc);

%% Divergence of the velocity field (xi)
%calcualte and graph divergence of velocity field
fc = div_calc(length_y,t,Mf, sigmaf, fc);

%% Hamiltonian
%calculate and graph potential, kinetic, and total energy
fc = energy_calc(length_y,t, Mf, sigmaf, fc,rho,G);
```

7.2 MatrixToVector function

```
function yout = matrixToVector(sigma, M)
y(1) = M(1,1);
y(2) = M(1,2);
y(3) = M(1,3);
y(4) = M(2,1);
y(5) = M(2,2);
y(6) = M(2,3);
y(7) = M(3,1);
y(8) = M(3,2);
y(9) = M(3,3);
y(10) = sigma(1,1);
y(11) = sigma(1,2);
y(12) = sigma(1,3);
y(13) = sigma(2,2);
y(14) = sigma(2,3);
y(15) = sigma(3,3);

yout = y';  % put all transposes inside the subroutine
end
```

7.3 VectorToMatixCell function

```
function [Mf, sigmaf] = vectorToMatrixCell(y)

size_y = size(y);
length_y = size_y(1,1);
Mf = cell(length_y,1);
sigmaf = cell(length_y,1);

for i = 1:length_y
    Mf{i} = [y(i,1) y(i,2) y(i,3); y(i,4) y(i,5) y(i,6);...
        y(i,7), y(i,8), y(i,9)];
    sigmaf{i} = [y(i,10) y(i,11) y(i,12); y(i,11) y(i,13) y(i,14);...
        y(i,12), y(i,14), y(i,15)];

end

end
```

7.4 Get axes function

```
function [Rf, a, b, c] = get_axes(length_y, sigmaf, rho)
volume = 4/3*pi;
Rf{length_y} = cell(1,length_y);
Df{length_y} = cell(1,length_y);
a = zeros(length_y,1);
b = zeros(length_y,1);
c = zeros(length_y,1);

for j = 1:length_y
    [Rf{j}, Df{j}] = eig(sigmaf{j});
    c(j) = (Df{j}(1,1)*5/(rho*volume))^0.5;
    b(j) = (Df{j}(2,2)*5/(rho*volume))^0.5;
    a(j) = (Df{j}(3,3)*5/(rho*volume))^0.5;
end

end
```

7.5 Volume calculation function

```
function [Vol fc] = volume_calc(length_y, t, at, bt, ct,fc)

Vol = zeros(length_y,1);

for i = 1:length_y
    Vol(i) = (4*pi/3)*at(i)*bt(i)*ct(i);
end

figure(fc)
fc = fc + 1;
plot(t, Vol)
title('Total Volume')

end
```

7.6 Plot axes function

```
function fc = plot_axes(t,at,bt,ct,fc)

figure(fc)
plot(t,at,'r')
hold on
plot (t,bt,'g')
hold on
plot (t,ct,'b')
title('Lengths of axes over time')
legend('a','b','c')
hold off
fc = fc+1;

end
```

7.7 Gamma calculation function

```
function fc = gamma_calc(length_y,t,Mf, sigmaf, fc)

gamma_squared = zeros(1,length_y);

for j = 1:length_y
    gamma_squared(j) = trace(inv(sigmaf{j})*Mf{j}*sigmaf{j}*(Mf{j})'...
        - Mf{j}*Mf{j});
end

figure(fc);
fc = fc +1;
plot(t,gamma_squared);
title('gamma squared')
end
```

7.8 Divergence calculation function

```
function fc = div_calc(length_y,t,Mf, sigmaf,fc)

xi = zeros(1,length_y);
for j = 1:length_y
```

```
    xi(j) = trace(inv(sigmaf{j})*Mf{j});
end

figure(fc)
fc = fc + 1;
plot(t,xi)
title('xi: Divergence of the Velocity Field')

end
```

7.9 Energy calculation function

```
function fc = energy_calc(length_y,t, Mf, sigmaf, fc,rho,G)

[¬,at,bt,ct] = get_axes(length_y, sigmaf, rho);

% kinetic energy
KE = zeros(length_y,1);
for i = 1:length_y
    KE(i) = 1/2*trace(Mf{i}'*inv(sigmaf{i})*Mf{i});
end

% Self-gravitating potential energy
I = zeros(length_y,1);
V = zeros(length_y,1);
E = zeros(length_y,1);
for i = 1:length_y
    func = @(x) 1./sqrt((at(i).^2+x).*(bt(i).^2+x).*(ct(i).^2+x));
    I(i) = integral(func, 0, Inf, 'RelTol',1e-12,'AbsTol',1e-12);
    V(i) = - 3/10*(rho.*4/3*pi*at(i).*bt(i).*ct(i))^2*G.*I(i);
    %V(i) = 3/10*(4/3*pi*at(i)*bt(i)*ct(i)).^2*rho*G*I(i);
    E(i) = KE(i) + V(i); %E is total energy
end

%graph of total energy
figure(fc)
fc = fc + 1;
plot(t,E)
title('Total Energy')

%graph of potential energy

figure(fc)
fc = fc + 1;
plot(t,KE,'r')
hold on
title('Kinetic Energy (red) and Potential Energy (blue)')
plot(t,V, 'b')
hold off

end
```

8 Acknowledgement

I would first like to thank my thesis advisor, Prof. Biello, who provided me help when I encountered any mathematical problems and also guided us on programming to visualize our results.

I would also like to thank my colleague, Polina Khapikova, who studied this topic with me and helped me a lot with coding. The codes which I post in the previous section is mainly her and Prof. Biello's work. Without their helps, I would not be able to get to where I am so far.

References

[1] S. Chandrasekhar, *Ellipsoidal figures of equilibrium*, Dover Publications, Inc., New York, 1987.

[2] P.J. Morrison, N.R. Lebovitz, J.A. Biello, *The hamiltonian description of incompressible fluid*, Ann. Phys. vol. 324 (2009), no. 8, 1747-1762, doi: 10.1016/j.aop.2009.04.003

[3] R.M. Roberts, M.E.R. Sousa Dias, *Symmetries of Riemann ellipsoids*, Resenhas IME-USP. vol. 4 (1999), no. 2, 183-221.

[4] G. Rosensteel, *Rapidly rotating nuclei as Riemann Ellipsoids*, Ann. Phys. vol. 186 (1988), no. 2, 230-291, doi: 10.1016/0003-4916(88)90002-4